

Disorder-driven intermediate state in the lattice melting transition of $\text{Bi}_2\text{Sr}_2\text{CaCu}_2\text{O}_{8+\delta}$ single crystals

A. Oral, J. C. Barnard, and S. J. Bending

Department of Physics, Faculty of Science, University of Bath, Bath BA2 7AY, United Kingdom

S. Ooi, H. Taoka, and T. Tamegai

Department of Applied Physics, The University of Tokyo, Tokyo 113, Japan

M. Henini

Department of Physics, University of Nottingham, Nottingham NG7 2RD, United Kingdom

(Received 3 September 1997)

Scanning Hall probe microscopy has been used to study high quality single crystals of the $\text{Bi}_2\text{Sr}_2\text{CaCu}_2\text{O}_{8+\delta}$ high-temperature superconductor over a wide range of temperatures at low fields. We observe pronounced stripes of high flux density which persist well above the melting line almost up to the critical temperature of the crystal. We show that these regions impose a disorder-driven intermediate state on the vortex lattice melting transition with a structure composed of alternating solid and liquid strips. We propose that the striping may reflect regions of slightly different oxygen doping level formed due to enhanced diffusion at the edges of atomic terraces during crystal growth. We are unable to resolve discrete vortices in the stripes above the vortex lattice melting line. We speculate either that the vortex liquid efficiently screens any pinned flux present or that spatial variations in the Gibbs free energy may be imposing a density modulation on the vortex liquid at these temperatures. [S0163-1829(97)51946-1]

High- T_c $\text{Bi}_2\text{Sr}_2\text{CaCu}_2\text{O}_{8+\delta}$ (BSCCO) single crystals have been extensively studied in recent years since their strong crystalline anisotropy gives rise to a very rich magnetic field-temperature phase diagram. Controversy still surrounds some regions of this diagram, but there is broad consensus that the vortex line solid melts at a well-defined field and temperature dependent phase boundary,¹⁻⁴ although whether the lines decouple to a liquid of flux pancakes exactly at the melting line⁵ or at a slightly higher temperature⁶ is still contentious. Furthermore the observation of sharp jumps in bulk magnetization³ and local induction⁴ measurements at the melting transition suggest that it may be of first order. We have performed high resolution scanning Hall probe measurements of flux distributions in high quality BSCCO crystals over a wide range of fields and temperatures and, below the melting line, observe small amounts of strongly pinned flux in all samples. Moreover the trapped flux is clearly seen to lie in stripes running approximately parallel to one of the crystallographic axes, separated by regions free of strong pinning sites. Surprisingly these stripes are still observable just below T_c , well above the vortex lattice melting temperature. Since the field corrugation associated with the striping is small (~ 1 G) one might expect them to be of no major significance, yet we show directly that they have a profound influence on the spatial structure of the lattice melting transition.

The design of our scanning Hall probe microscope (SHPM) has been described in detail elsewhere.⁷ In brief the Hall probe has an effective spatial resolution of $\sim 0.8 \mu\text{m}$ and is patterned in a GaAs/AlGaAs heterostructure two-dimensional electron gas about $13 \mu\text{m}$ from the corner of an etched mesa which is coated with a thin layer of gold to act as a scanning tunneling microscope (STM) tip. The BSCCO

crystal is mounted on the sample puck of a commercial low temperature STM and a stick-slip coarse translation mechanism used to approach the sensor which is fixed directly to the end of the piezo scanner tube. The sample is tilted $1-2^\circ$ with respect to the Hall probe to ensure that the STM tip is always the closest point to it. The most convenient scanning mode is with the Hall probe lifted away from the sample surface by a fraction of a micron and any remaining tilt angle between the crystal face and the scanner plane can be measured in STM mode and electronically compensated during such scans. The entire microscope assembly sits at the center of a commercial temperature-controlled cryostat incorporating a double stage vibration isolation system.

The high quality as-grown BSCCO crystals investigated here were prepared by the traveling solvent floating zone technique.⁸ Crystal *A* had approximate dimensions $3 \text{ mm} \times 2 \text{ mm} \times 100 \mu\text{m}$ while crystal *B* was slightly smaller ($\sim 2 \text{ mm} \times 2 \text{ mm} \times 100 \mu\text{m}$) and in both cases T_c was estimated to be about 90.5 K from an extrapolation of the melting line to zero field. This agreed well with the temperature at which the striping described here disappeared. A second smaller crystal from the same batch as crystal *A* was also investigated in a different cryostat using a static Hall probe array with $2 \mu\text{m}$ resolution to establish an independent estimate of the melting line.

Figure 1(a) shows an SHPM image of a region near the center of crystal *A* after field cooling to 77 K in 2.1 Oe, while a 2.5 Oe field cooled image from crystal *B* is shown in Fig. 1(b). Note that in both samples the vortices (bright circles) appear to lie on pronounced stripes, separated by flux free regions, which run approximately parallel to one of the crystallographic axes as shown with a spacing of $\sim 10 \mu\text{m}$.

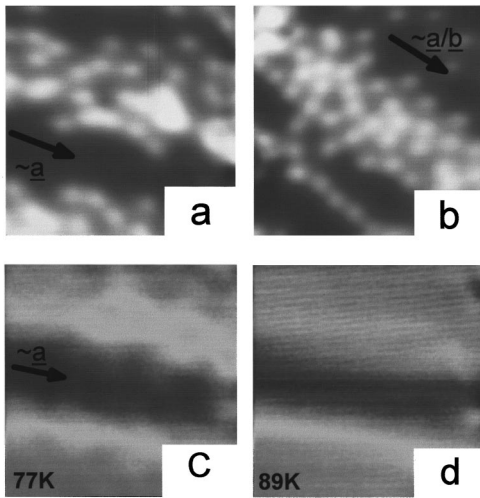


FIG. 1. SHPM images of (a) crystal *A* after field cooling to 77 K in 2.1 Oe (grayscale spans 3.18 G), (b) crystal *B* after field cooling to 77 K in 2.5 Oe (grayscale spans 3.73 G), (c) crystal *A* after field cooling to 77 K in 30 Oe (grayscale spans 0.73 G), and (d) sample shown in (c) after heating to 89 K (grayscale spans 0.60 G). Arrows indicate the approximate direction of the crystal *a* axis ($\sim a$) or for (b) the *a* or *b* axes ($\sim a/b$). Image size is $\sim 25 \mu\text{m} \times 25 \mu\text{m}$ in all cases.

For crystal *A* x-ray analysis revealed that the direction of the stripes approximately coincides with the *a* axis, while on the basis of the shape of crystal *B* we estimate that it is close to either the *a* or *b* axes. Integration of the flux associated with the well-resolved bright circles yields about 95% of a flux quantum consistent with their identification as superconducting vortices. In the regions of highest flux density individual vortices can no longer be resolved due to the finite spatial resolution of our SHPM. We have made a number of measurements of different regions of the crystals and similar striping has been seen at every location. It was also observed after small amounts of material were cleaved from the top of crystal *A* to create a clean surface, although the relatively coarse in-plane SHPM alignment mechanism prevents us from demonstrating that the locations remain unchanged. A careful analysis of the vortex positions within the stripes indicates that they are fairly homogeneously distributed although a pronounced tendency for chain formation is evident in Fig. 1(b). At higher applied fields we eventually lose single vortex resolution entirely and the regions of strong pinning manifest themselves as corrugations in the local magnetic induction profile as shown in Fig. 1(c) for crystal *A* after field cooling to 77 K in 30 Oe. This shows the same area of the sample as Fig. 1(a) but after a different cooling cycle on a different day and the regions between the bright stripes do now contain vortices. Figure 1(d) shows a subsequent image of the same region after the temperature has been raised to 89 K and note that the striping is still observed although the corrugation has a weaker amplitude. It is certainly surprising that we find pronounced microscopic flux inhomogeneity at such a high temperature which is well above the melting line (~ 84 K at this field) although we emphasize that the corrugation only represents about 2% of

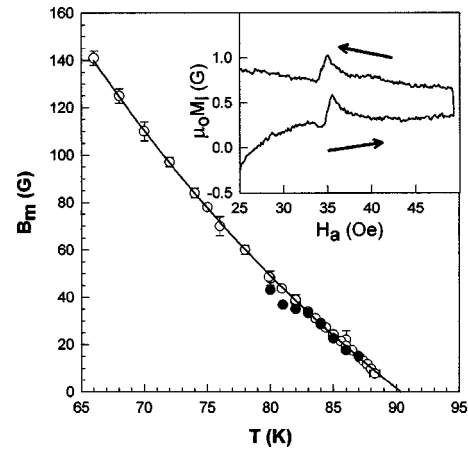


FIG. 2. Melting line measured with the SHPM for crystal *A* (solid circles) and by static Hall probe magnetometry on a crystal from the same growth batch (open circles). Inset shows typical local magnetization construction for crystal *A* at 82 K.

the total induction in Fig. 1(d). As one would expect the striping eventually disappears above the critical temperature of the crystal.

Static local magnetic induction measurements were performed on the smaller crystal from the same batch as sample *A* in a separate cryostat. Clear induction jumps at the lattice melting transition were observed⁴ and used to construct the phase line as shown in Fig. 2 (open circles). The slope of this line conforms well to that measured in high quality as-grown crystals by other authors.⁹ For comparison the local induction was measured in the SHPM with the Hall probe held fixed about $5 \mu\text{m}$ above the surface of crystal *A* to smear out fine structure due to discrete vortices moving under the sensor. A typical local magnetization measurement ($\mu_0 M_l = B - \mu_0 H_a$) is shown in the inset of Fig. 2 and also shows a very clear jump at the melting line. Note that the data is presented in this way for clarity and there is no direct relation between this quantity and the thermodynamic bulk magnetization. The small irreversibility in this trace is probably due to the existence of geometric barriers at the edges of our platelet-shaped samples as discussed in some detail in Ref. 10. The melting induction (B_m) measured in this way at a few different temperatures has been added to the data in Fig. 2 (solid circles) and agrees well with the results from the smaller crystal given that the field calibration of the two cryostats used could differ by a few percent.

Crystal *A* was now zero-field cooled to 82 K and the Hall probe approached to within a fraction of a micron from the crystal surface. After positioning at various strategic locations as indicated by the letters in the SHPM image of Fig. 3(a) local magnetization traces were again measured and these are presented in Fig. 3(b). No attempt was made to field cool the sample again after each trace had been obtained since this would lead to undesirable thermal drifts in the location of the Hall probe as well as its elevation above the sample. The local induction data were instead captured after several hysteresis cycles at each site so that each trace has almost exactly the same magnetic history. Note that a clear induction jump is seen at all locations in the image, but it occurs at significantly lower applied fields in the bright stripe regions than in the lower induction strips between them.

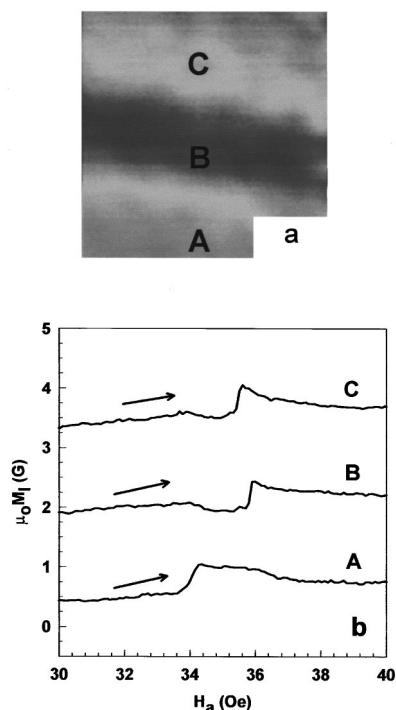


FIG. 3. (a) SHPM image of crystal A after field cooling to 82 K at 38 Oe (grayscale spans 0.81 G and image size is $\sim 25 \mu\text{m} \times 25 \mu\text{m}$). (b) Family of 82 K local magnetization traces at the three locations in the image indicated by the letters A–C.

Moreover the entire melting transition spans an applied field range of ~ 2 Oe, which is about four times larger than the field corrugation at this temperature.

Similar data are more graphically presented in Fig. 4 where four 81 K SHPM images are shown at different applied fields through the melting transition. Again, in order to avoid thermal drifts in the Hall probe position the sample was not field cooled at each value of applied field. Instead, only the image at 38 Oe was field cooled after which the value of H_a was simply increased as required. Since the changes in contrast in these images are fairly subtle, line scans in the indicated direction perpendicular to the striping are also included and each curve has been offset vertically for clarity. At 38 Oe the sample has not yet begun to melt and we measure the intrinsic field corrugation. At 38.5 Oe the brightest stripe at the bottom of the image is beginning to melt as evidenced by the appreciably larger induction at this edge. At 40 Oe the stripes near the top and bottom of the image have now melted while the strip in the middle remains untransformed. This situation clearly gives rise to the strongest corrugation that one can observe which is about 0.4 G higher than in the solid state. Finally at 40.5 Oe the strip in the middle has also melted, and the line scan as well as the overall image is almost indistinguishable from that of the vortex solid at 38 Oe. This is quite remarkable since one would expect the vortex system to behave completely differently on either side of the melting line.

Although all our measured parameters point to the high quality of our crystals it is important to look for any other indications that they may be atypical. To this end magneto-optical imaging of flux penetration into crystal A has been performed after removal from the SHPM sample puck. At

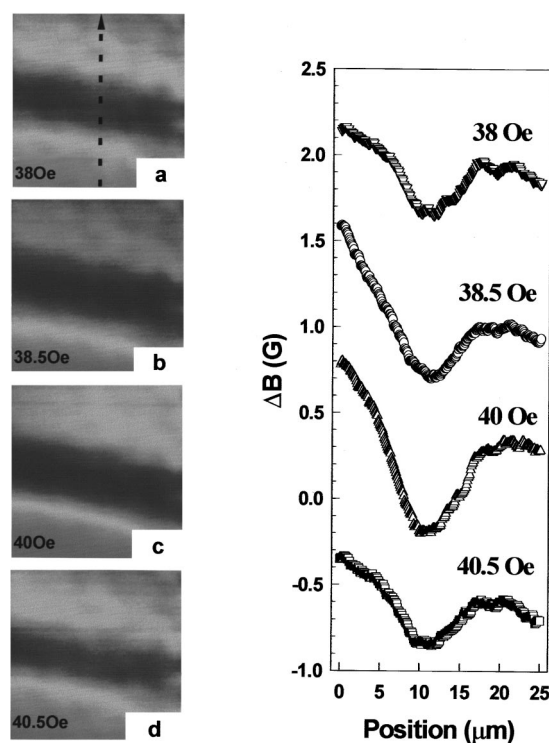


FIG. 4. SHPM images of crystal A at 81 K in applied fields of (a) 38 Oe (grayscale spans 0.81 G), (b) 38.5 Oe (grayscale spans 1.02 G), (c) 40 Oe (grayscale spans 1.18 G), and (d) 40.5 Oe (grayscale spans 0.84 G). Image size is $\sim 25 \mu\text{m} \times 25 \mu\text{m}$ in each case. Also shown are line scans at the four different fields in the direction indicated.

low temperatures ($T \leq 20$ K) flux entry at applied fields up to 1000 Oe does show coarse scale (~ 0.5 mm) irregularity along two edges of the crystal which can be traced to the presence of three deep scratches beneath one side and a rough edge profile on the other. Flux entry is, however, rather uniform along the other two edges where some of our images have been obtained and we do not believe that such coarse structure is related to the striping reported here.

The observation of strongly pinned flux in any of our images is at first sight surprising since a low field depinning line (near $T \sim 30$ K) has recently been identified in these materials associated with a sharp feature in the logarithmic derivative of the magnetic moment with respect to temperature which is almost field independent.¹¹ In practice, however, this line represents a crossover from strong to weak pinning and not to zero pinning. It seems that there may be two characteristic types of disorder in these crystals; one that is more pointlike and only effective below the depinning line and one that is more extended along the c axis (i.e., closer to columnar defects) and gives rise to the striping seen here. The fact that the stripes appear to lie along one of the crystallographic axes (a axis in crystal A and either a or b axes in crystal B) leads us to speculate that they may be correlated with the location of the edges of atomic terraces at some point during crystal growth where oxygen diffusion is known to be enhanced. In addition Li *et al.*¹² have recently reported strong in-plane anisotropy for oxygen out-diffusion from BSCCO single crystals, being 5–6 times faster along the a axis than the b axis, and this could very well be a contribu-

tory factor in stripe formation. Thus strips of different contrast may represent regions of slightly different oxygen stoichiometry, although a more detailed picture of the mechanism giving rise to them remains unclear. Recent local induction studies⁹ have demonstrated that the position of the melting line depends quite sensitively on oxygen content and would imply that the high induction stripes may then represent regions where doping is closer to optimal.

The existence of striping up to temperatures just below T_c is certainly remarkable since this is well above both the melting (and decoupling) line at the fields in question. We have recently increased the spatial resolution of our SHPM to $\sim 0.2 \mu\text{m}$ in order to make a vortex-resolved study of the melting transition in these materials.¹³ In the course of these experiments we have never been able to image discrete vortices above the melting line although they are quite well resolved beneath it. We therefore have no direct evidence that the high-temperature stripes correspond to regions of pinned vortices. It is possible that the vortex liquid effectively screens any pinned vortices present making them invisible to our experiment. Alternatively we speculate that a better way to view the problem may be to consider the striping as corresponding to corrugations of the Gibbs free energy which in turn impose density modulations on the vortex liquid. We note, however, that the structure and contrast of the stripes below and well above the melting line are extremely similar, and it is not at all clear that this is to be expected from the second picture.

Finally we note that the measurements we report here correspond to the observation of an intermediate state of alternating melted and solid strips of superconductor as proposed by Farrell *et al.*,¹⁴ although one driven by inhomogeneities rather than thermodynamics. Such microscopic striping certainly suppresses any tendency for a thermodynamic intermediate state to form and an extremely homogeneous crystal would be required to observe this. It is well known that surface/geometrical barriers give rise to a dome-like flux distribution in BSCCO single crystal platelets and the magnetic induction is typically $\sim 4 \text{ G}$ higher in the sample center than at the edge.¹⁵ As a consequence the melting transition begins at the crystal center and works its way out to the edges with increasing applied field. When we combine this fact with our observation that the stripe melting transition spans an applied field range of $\sim 2 \text{ Oe}$ we would expect a large part of the sample to be in this intermediate state at any time, and the melt should assume the form of

extremely long $\sim 10 \mu\text{m}$ wide fingers directed out towards the crystal edges. We do not think that there is any conflict with the observation in Ref. 4 that the breadth of the local induction jumps is less than 0.4 G since $3 \mu\text{m}$ wide Hall probes were used there. This is somewhat smaller than the typical dimensions of a stripe and there is no reason why the jump should not be very sharp indeed. One might anticipate that the induction jump would be broadened to $\sim 2 \text{ Oe}$ in measurements with larger Hall probes ($\geq 20 \mu\text{m}$) which average over more than one stripe and this does appear to be the case. Bitter decoration experiments have shown that surface steps can act as pinning centers for vortices in BSCCO provided they are substantially higher than $\sim 30 \text{ nm}$ at a measurement field of 33 Oe .¹⁶ AFM investigations of our crystals revealed no cracks and no surface steps higher than 10 nm (apart from the three already mentioned) so such a mechanism can be discounted here. We also emphasize that the ability to generate highly ordered decoration images on BSCCO crystals over large areas would not be significantly compromised since at typical fields ($\sim 70 \text{ Oe}$) the striping corresponds to a modulation of less than 0.4% in the vortex lattice spacing.

In conclusion we have shown that high quality as-grown BSCCO single crystals contain stripes of pinned flux which persist up to the lattice melting temperature. The stripes tend to lie along one of the in-plane crystallographic axes (probably the a axis) of the crystal and may represent regions of different doping level formed due to enhanced oxygen diffusion at the edges of atomic terraces during crystal growth. Although the levels of trapped flux are very small they have a profound effect on the spatial structure of the melting transition and we are able to show the presence of a disorder-driven intermediate state in the transformation region. Surprisingly the striping is still observed well above the vortex lattice melting temperature although we have no direct evidence that flux is actually pinned at these temperatures. We speculate either that the vortex liquid efficiently screens trapped flux present or that spatial variations in the Gibbs free energy may, in turn, impose a density modulation on the vortex liquid in this regime.

The authors wish to thank Professor D. E. Farrell for useful discussions. This work was supported in the United Kingdom by EPSRC and MOD Grant No GR/J03077 and the University of Bath through the initiative fund as well as a grant-in-aid for scientific research from the Ministry of Education, Science, Sports and Culture in Japan.

¹S. L. Lee *et al.*, Phys. Rev. Lett. **71**, 3862 (1993).

²R. Cubitt *et al.*, Nature (London) **365**, 407 (1993).

³H. Pastoriza *et al.*, Phys. Rev. Lett. **72**, 2951 (1994).

⁴E. Zeldov *et al.*, Nature (London) **375**, 373 (1995).

⁵D. T. Fuchs *et al.*, Phys. Rev. B **55**, R6156 (1997).

⁶C. D. Keener *et al.*, Phys. Rev. Lett. **78**, 1118 (1997).

⁷A. Oral *et al.*, Appl. Phys. Lett. **69**, 1324 (1996).

⁸N. Motohira *et al.*, J. Ceram. Soc. Jpn. **97**, 994 (1989).

⁹B. Khaykovich *et al.*, Phys. Rev. Lett. **76**, 2555 (1996).

¹⁰D. Majer *et al.*, Phys. Rev. Lett. **75**, 1166 (1995).

¹¹C. D. Dewhurst and R. A. Doyle, Phys. Rev. B **56**, 10 832 (1997).

¹²T. W. Li *et al.*, Physica C **224**, 110 (1994).

¹³A. Oral, J. C. Barnard, S. J. Bending, S. Ooi, T. Tamegai, I. I. Kaya, and M. Henini (unpublished).

¹⁴D. E. Farrell *et al.*, Phys. Rev. B **53**, 11 807 (1996).

¹⁵E. Zeldov *et al.*, Europhys. Lett. **30**, 367 (1995).

¹⁶S. W. Yoon *et al.*, Science **265**, 215 (1994).